

514-10  
1994

**N95- 32432**

**IMPLEMENTATION OF A SINGLE-STAGE-TO-ORBIT (SSTO)  
MODEL FOR STABILITY AND CONTROL ANALYSIS**

**Final Report  
NASA/ASEE Summer Faculty Fellowship Program--1994  
Johnson Space Center**

<b>Prepared By:</b>	<b>Stephen A. Ingalls, MSAE</b>
<b>Academic Rank:</b>	<b>Assistant Professor</b>
<b>College and Department:</b>	<b>United States Military Academy Department of Civil and Mechanical Engineering West Point, New York 10996</b>
<b>NASA/JSC</b>	
<b>Directorate:</b>	<b>Engineering</b>
<b>Division:</b>	<b>Navigation, Control, and Aeronautics</b>
<b>Branch:</b>	<b>Control and Guidance</b>
<b>JSC Colleague:</b>	<b>G. Gene McSwain</b>
<b>Date Submitted:</b>	<b>August 5, 1994</b>
<b>Contract Number:</b>	<b>NGT-44-005-803</b>

The tendency to combine the three metrics into one will only obscure information and should be avoided. The recommendation that each of the three be tracked separately is yet another reason to restricting ourselves to three metrics.

It is fully expected that each IPT will avail themselves of sophisticated methods to establish the value of the parameters. It may well even be true that each IPT uses a different method. However, over time and with experience, it is reasonable to suppose that some methods will prevail and become common. Here, the intent is to let use determine the method as opposed to method determining the use.

#### Step 4: Reconciliation

The top ten plus one list should be compared to the three metrics generated to see if the information plays well together. Logic and consistency are important. In essence, the IPT has verified their feelings on risk by working the problem two different ways, one in paragraph form and the other with the metrics. This part of the report should be in paragraph form and discuss how the two different parts support each other.

#### Step 5: Transition

Risk management is dynamic. The RM plan requires a periodic review to insure it is meeting its required objectives and to insure that the objectives themselves have not changed. As the program becomes more operational in nature, significant changes in the definition of success will occur forcing changes in the IRM plan. Step 5 in the report is a paragraph discussing how the office plans to deal with the change from a risk perspective.

## CONCLUSIONS

As was stated earlier in the paper, this is a tentative beginning of the development of the foundations of risk management. Surely significant changes and modifications will occur with time. The question now becomes one of whether the implementation of such a program is worth the overhead that it brings. Can a program afford to implement an IRM plan?

One of the problems with technical decision making is that non-technical people understand neither the principles involved nor the process. Given this, they have to trust the technocrat to do what is right and correct. One thing is resoundingly clear, if the community as a whole loses their faith in the technocrats to make the "good" decision, they can shut the whole process down. If Congress loses its faith in NASA, they can stop the space station. If the public loses its faith in a company, they can force financial ruin. If the auditors and accountants lose their faith in the design team they can stop a project.

Given this and given the high risk of many technical decisions, the question more properly becomes one of can a company or program afford not to institute a formal risk management plan?

high-performance aircraft are purposely designed statically unstable, increasing their maneuverability. Instabilities are easily controlled using feedback: pilot-in-the-loop, automatic flight control systems, or both.

Dynamic stability is the time-response of an aircraft to a perturbation. Dynamic instability is also acceptable in an aircraft, presuming the divergence from an equilibrium condition is slow enough. These instabilities are also dealt with using human or automatic feedback.

### **Moment Trim**

Separate from, yet related to, stability is moment trim. For an aircraft to achieve an equilibrium flight condition, moments about the center of gravity, both longitudinally and laterally, must balance. This balance is dependent on static stability derivatives and control effectiveness, measured in terms of control derivatives, useful aerodynamic angles of attack, and maximum allowed deflections. An altitude and airspeed where moment trim is not achievable is an infeasible flight condition, regardless of the level of static or dynamic stability.

## DISCUSSION

### Static Stability

Rather than look at every force and moment response to every input motion variable, an arbitrary set of static stability criterion is established:

- Velocity disturbances are initially opposed only by forces.
- Rotational velocity disturbances are initially opposed only by moments.
- Angle of attack and sideslip disturbances obtained by interpreting the velocity disturbances  $v$  and  $w$  as  $\beta = v/U_1$  and  $\alpha = w/U_1$  are initially opposed only by moments.

Static stability is indicated when the *initial* response of the vehicle is a return toward the equilibrium point.

The change in side-force coefficient,  $C_Y$ , with change in sideslip angle,  $\beta$ , serves to illustrate the shorthand notation used with stability derivatives:

$$\frac{\partial C_Y}{\partial \beta} = C_{Y\beta} \quad (1)$$

The criteria for static stability are outlined in Table 1.

TABLE 1.- AIRPLANE STATIC STABILITY CRITERIA

Forces and Moments	Perturbed Variable							
	u	v	w	$\beta = v/U_1$	$\alpha = w/U_1$	p	q	r
Drag + X-Thrust	$C_{Du} > 0$							
Sideforce + Y-Thrust		$C_{Y\beta} < 0$						
Lift + Z-Thrust			$C_{L\alpha} > 0$					
Roll Moment + Roll-Thrust				$C_{l\beta} < 0$		$C_{lp} < 0$		
Pitch Moment + Pitch-Thrust	$C_{mu} > 0$				$C_{m\alpha} < 0$		$C_{mq} < 0$	
Yaw Moment + Yaw-Thrust				$C_{n\beta} > 0$				$C_{nr} < 0$

As current work concentrates on the descent-to-land mission phase (the aircraft is in unpowered, gliding flight), thrust forces of Table 1 are not considered. The only derivative contrary to our rules is the pitching moment response to a linear velocity,  $C_{mu}$ . Inclusion is a function of its physical significance.

## Static Stability Results

Where possible, stability derivatives were determined directly from the LaRC aerodynamic database by applying a forward differencing method between available data points. Curve-fits were applied to data which was highly non-linear with the perturbed variable of interest (drag with angle of attack and longitudinal forces and moments with u-velocity (Mach number)). Results of this analysis are presented in Table 2.

TABLE 2.- WB001 STATIC STABILITY

Forces and Moments	Perturbed Variable							
	u	v	w	$\beta = v/U_1$	$\alpha = w/U_1$	p	q	r
Drag	STABLE							
Sideforce		STABLE						
Lift			STABLE					
Roll Moment				NOTE 2		STABLE		
Pitch Moment	NOTE 1				STABLE		STABLE	
Yaw Moment				NOTE 3				STABLE

Note 1: This SSTO variant exhibits a tendency to tuck its nose with increasing velocity ( $C_{mu} < 0$ ) for angles of attack greater than 3.25 degrees (Mach = 0.30) and at  $\alpha$ s greater than -8.04° at Mach = 0.60.

Note 2: Dihedral effect ( $C_{l\beta}$ ) is unstable (positive) at Mach 0.30 and angles of attack less than 12.0 degrees. For Mach = 0.60, the vehicle is statically unstable at less than 10.0 degrees  $\alpha$ .

Note 3: WB001 is statically unstable for all flight conditions studied.

## Moment Trim

The six degrees of freedom available to an aircraft are represented by six equations of motion (conservation of linear and angular momentum). Modeling aerodynamic forces as a first-order Taylor Series expansion and writing the equations for rectilinear flight yields:

$$\begin{aligned}
 mg \sin \gamma &= -(C_{D_o} + C_{D_\alpha} \alpha + C_{D_{\delta_{bf}}} \delta_{bf} + C_{D_{\delta_e}} \delta_e + C_{D_{\delta_{tf}}} \delta_{tf}) \bar{q} S \\
 -mg \sin \phi \cos \gamma &= (C_{Y_o} + C_{Y_\beta} \beta + C_{Y_{\delta_{ail}}} \delta_{ail} + C_{Y_{\delta_{tf}}} \delta_{tf}) \bar{q} S \\
 mg \cos \phi \cos \gamma &= (C_{L_o} + C_{L_\alpha} \alpha + C_{L_{\delta_{bf}}} \delta_{bf} + C_{L_{\delta_e}} \delta_e + C_{L_{\delta_{tf}}} \delta_{tf}) \bar{q} S \\
 0 &= C_{l_\beta} \beta + C_{l_{\delta_{ail}}} \delta_{ail} + C_{l_{\delta_{tf}}} \delta_{tf} \\
 0 &= C_{m_o} + C_{m_\alpha} \alpha + C_{m_{\delta_{bf}}} \delta_{bf} + C_{m_{\delta_e}} \delta_e + C_{m_{\delta_{tf}}} \delta_{tf} \\
 0 &= C_{n_\beta} \beta + C_{n_{\delta_{ail}}} \delta_{ail} + C_{n_{\delta_{tf}}} \delta_{tf}
 \end{aligned} \tag{2}$$

Further modification to these equations is possible by assuming zero bank angle,  $\phi = 0$ . This substitution decouples the longitudinal set of equations from the lateral and is representative of actual mission profiles flown from 10,000 feet to the runway.

### Longitudinal Equations of Motion

$$\begin{aligned}
 mg \sin \gamma &= -(C_{D_o} + C_{D_\alpha} \alpha + C_{D_{\delta_{bf}}} \delta_{bf} + C_{D_{\delta_e}} \delta_e + C_{D_{\delta_{tf}}} \delta_{tf}) \bar{q} S \\
 -mg \cos \gamma &= (C_{L_o} + C_{L_\alpha} \alpha + C_{L_{\delta_{bf}}} \delta_{bf} + C_{L_{\delta_e}} \delta_e + C_{L_{\delta_{tf}}} \delta_{tf}) \bar{q} S \\
 0 &= C_{m_o} + C_{m_\alpha} \alpha + C_{m_{\delta_{bf}}} \delta_{bf} + C_{m_{\delta_e}} \delta_e + C_{m_{\delta_{tf}}} \delta_{tf}
 \end{aligned} \tag{3}$$

In these equations, flight path angle ( $\gamma$ ), angle of attack ( $\alpha$ ), body-flap deflection ( $\delta_{bf}$ ), elevator deflection ( $\delta_e$ ), and tip-fin deflection ( $\delta_{tf}$ ) are unknowns. Reducing the five unknowns to three is possible by first setting the body-flap deflection to zero, typically done for shuttle in the final stages of descent to ensure ground clearance at touchdown. Eliminating angle of attack dependency is possible by solving the set with LaRC aerodynamic characteristics for WB001 at each angle of attack from -10.0 to 20.0 degrees (subsonic range of useful  $\alpha$ ). The solution set:  $\gamma$ ,  $\delta_e$ , and  $\delta_{tf}$ , represents a longitudinal trim condition.

#### Lateral-Directional Equations of Motion

$$\begin{aligned} -mg \cos \gamma &= (C_{Y\beta} \beta + C_{Y\delta_{ail}} \delta_{ail} + C_{Y\delta_{tf}} \delta_{tf}) \bar{q} S \\ 0 &= C_{l\beta} \beta + C_{l\delta_{ail}} \delta_{ail} + C_{l\delta_{tf}} \delta_{tf} \\ 0 &= C_{n\beta} \beta + C_{n\delta_{ail}} \delta_{ail} + C_{n\delta_{tf}} \delta_{tf} \end{aligned} \tag{4}$$

In these equations, flight path angle ( $\gamma$ ), sideslip angle ( $\beta$ ), aileron deflection ( $\delta_{ail}$ ), and tip-fin deflection ( $\delta_{tf}$ ) are not known. Either the longitudinal flight path angle solution, or another flight path angle of interest, is substituted here, leaving three unknowns. It is important to differentiate tip-fin use in the longitudinal and lateral-directional cases. Tip-fins are employed for speed brake effect longitudinally and rudder effect laterally.

A trim solution does not guarantee feasibility. Maximum control deflections possible with the vehicle must exceed the solution obtained from these equation sets. Further, aerodynamic angles obtained must not exceed stall values in either  $\alpha$  or  $\beta$ .

#### Longitudinal Trim Results

A note concerning trim solutions for elevator deflection is warranted. WB001's control configuration is depicted in the schematic below (Figure 1). For these calculations, it was assumed both inboard and outboard panels were deflected to trim pitching moment. Obvious advantages in this are smaller control deflections (more surface area moving to counter the moment), resulting in decreased drag due to control movement and a greater percentage of available deflection to address dynamic stability concerns. Control derivatives for the elevator in equation sets 2 and 3 above are, therefore, the addition of drag, lift, and pitching moment derivatives with respect to both aileron and elevon movement. Longitudinal trim results are shown in Figure 2.

Solutions at Mach 0.30 yield trim flight path angles on the order of 12 - 13 degrees (orbiter is  $\approx 20.0^\circ$ ) and angles of attack varying from around 17.8 degrees at 10,000 feet to 12.6 degrees at sea-level. These calculations presume a standard atmosphere. Trim angles of attack and elevator

deflection trend smaller at higher Mach number, while flight path angle increases to values in excess of 20 degrees at 10,000 feet. These data bound possible trim solutions and this effort does not design a final descent trajectory.

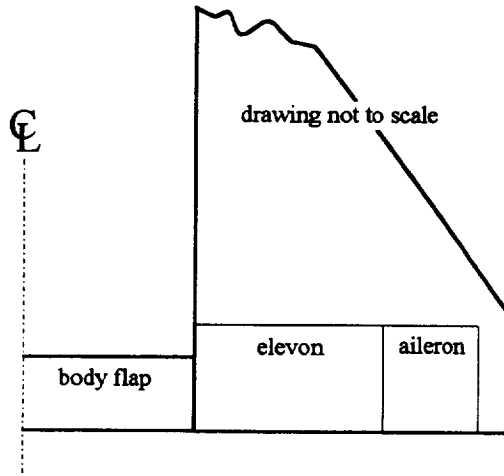


FIGURE 1.- WB001 CONTROL ORGANIZATION SCHEMATIC

### Lateral-Directional Trim Results

Lateral-directional trim was attempted in a similar manner. Rather than look at conditions throughout the final descent, trim was attempted for a design cross-wind condition at landing of 25 knots. Assuming touchdown velocities comparable to shuttle ( $\approx 200$  knots), this results in a design sideslip angle of approximately 7 degrees.

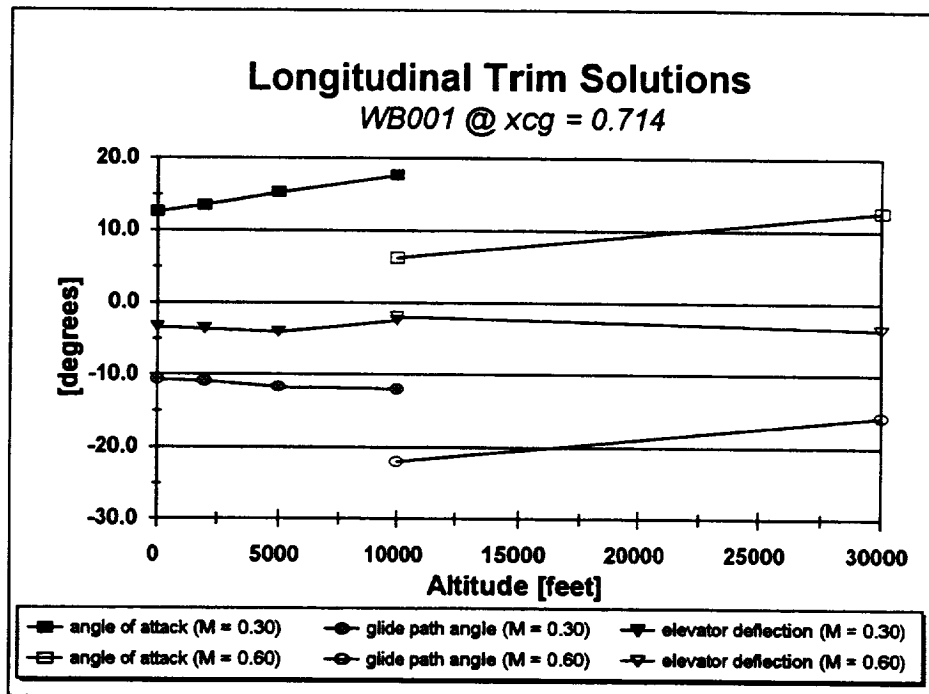


FIGURE 2.- LONGITUDINAL TRIM SOLUTIONS ( $\alpha$ ,  $\gamma$ , and  $\delta_e$ ) FOR TWO MACH NUMBERS VS. ALTITUDE



Further, orbiter design vertical velocities at touchdown are approximately 2.0 feet/second. Using this and the assumed touchdown velocity of around 200 knots results in a flight path angle of approximately zero ( $0.34^\circ$ ) for substitution into the lateral equation set.

Attempts to obtain a trim solution to the lateral equations of motion proved impossible, indicating the vehicle incapable of landing in the design cross-wind. This, coupled with  $C_{n\beta}$  static instabilities, suggested an analysis to improve the SSTO's inherent lateral stability.

### Tip-Fin Sizing

Early landing simulation of the SSTO indicated lateral divergence from design trajectories in both roll and yaw with small  $\beta$  (Figure 3). Further attempts to land the vehicle indicated increasing lateral force and moment effects resulted in more favorable performance. Discussions with engineers at LaRC indicated a pending effort to reevaluate tip-fin size.

Sizing lateral control surfaces to produce a desired  $C_{n\beta}$  derivative value is common practice in the preliminary design of aircraft. Considering vehicle weathercock stability ( $C_{n\beta}$ ) as a superposition of effects from the wing-body and lateral control surfaces, in this case, the tip-fins, yields:

$$C_{n\beta} = C_{n\beta\_wing-body} + C_{n\beta\_tip-fin} \quad (5)$$

The tip-fin contribution is further expressed as:

$$C_{n\beta\_tip-fin} = C_{L\alpha\_tip-fin} \left(1 - \frac{\partial \sigma}{\partial \beta}\right) \eta_{tf} \frac{S_{tf}}{S} \frac{X_{tf}}{b} \quad (6)$$

where,	$C_{L\alpha\_tip-fin}$	= Tip-Fin Lift-Curve Slope
	$\partial \sigma / \partial \beta$	= Change in Sidewash with Sideslip Angle
	$\eta_{tf}$	= Ratio of Dynamic Pressure at the Tip-Fin to the Wing
	$S_{tf}$	= Tip-Fin Surface Area [ft <sup>2</sup> ]
	$S$	= Wing Area [ft <sup>2</sup> ]
	$X_{tf}$	= Distance from Center-of-Gravity to Tip-Fin Aerodynamic Center [ft]
	$b$	= Wing Span [ft]

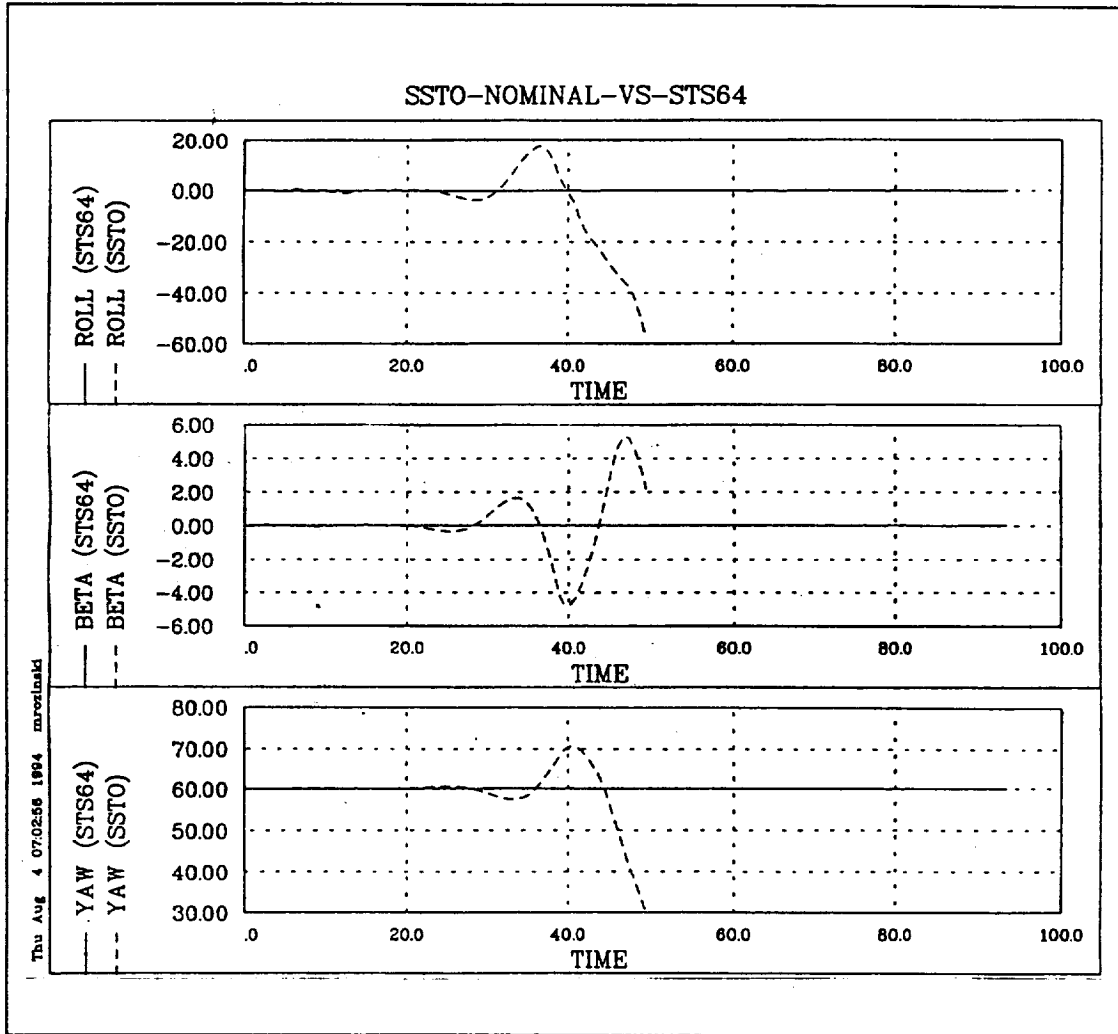


FIGURE 3.- SHUTTLE ENGINEERING SIMULATOR STRIP PLOTS COMPARING ROLL RATE [DEG/SEC], PITCH RATE [DEG/SEC] AND SIDESLIP ANGLE [DEG] VS. TIME [SECONDS] FOR THE SSTO TO ORBITER IN STS-64 CONFIGURATION

If we neglect sidewash dependence on  $\beta$  ( $\partial\sigma/\partial\beta$ ) and assume the dynamic pressure ratio ( $\eta_v$ ) is 1, equation 6 reduces to:

$$C_{n_{\beta\_tip-fin}} = C_{L_{\alpha\_tip-fin}} \frac{S_f}{S} \frac{X_f}{b} \quad (7)$$

$C_{L_{\alpha\_tip-fin}}$  was calculated as 2.174/radian using methods outlined in the United States Air Force Stability and Control Data Compendium

(DATCOM). Comparison of LaRC tip-fin yaw moment to tip-fin side force at the same deflection resulted in a value for  $X_{tf}$  (moment arm of the tip-fin control surface to vehicle center-of-gravity) of 56.112 feet. Substituting a wing area of 4,211 ft<sup>2</sup> and span equal to 95.72 ft, equation 7 shows how increasing tip-fin surface area results in a linear increase in  $C_{n\beta\_tip-fin}$ .

A vehicle  $C_{n\beta}$  of 0.100/radian was selected and is representative of the orbiter's subsonic lateral stability in this derivative. WB001's current tip-fin surface area is 214.95 ft<sup>2</sup>. Increasing area to obtain this degree of inherent stability requires a growth factor of 6.78 (total lateral control surface area required increases to 1,457 ft<sup>2</sup>).

This offers one method of improving vehicle lateral stability and cross-wind landing capability. Enhancing basic wing-body weathercock stability or employing alternative methods of improving tip-fin effectiveness without a size increase are equally viable options.

## CONCLUSIONS

This study concludes the WB001's current level of lateral stability is insufficient. In particular, lateral trim solutions for desired cross-wind components in the landing environment were not possible. Instabilities in roll and pitch 'tuck' also exist, but appear less significant than deficiencies in the  $C_{n\beta}$  derivative. Longitudinal trim solutions indicate steady-state glide path angles on the order of 12 degrees at Mach = 0.30, increasing to slightly greater than 20 degrees at M = 0.60. One attempt at improving the vehicle's lateral instabilities looked at sizing lateral control surfaces to a prescribed degree of inherent stability. A value comparable to subsonic stability of the orbiter ( $C_{n\beta} = 0.100/\text{radian}$ ) was selected and required increasing tip-fin surface area 6.78 times (from around 215 to 1,457 ft<sup>2</sup>). This carries a commensurate increase in aircraft weight, highly undesirable in a SSTO configuration. Other methods of enhancing the vehicle's lateral stability are available and require further study.

## REFERENCES

1. *Access to Space*. NASA Advanced Technology Team (Option 3), Volume 3. Final Report. 1993.
2. Englund, W. "SSV-001, 6-DOF Aero Database." Preliminary Aerodynamic Database. March 1994.
3. Hoak, D. E. et al. "USAF Stability and Control DATCOM." Data Compendium, 1978.
4. Lan, C. E. and J. Roskam. *Airplane Aerodynamics and Performance*. Roskam Aviation and Engineering Corporation, Ottawa, Kansas, 1988.
5. Lepsch, R. "Weight Statement - Level III, Unmanned SSV, Duel-Fuel, RD-701." Data Table, April 1994.
6. Rockwell International. "Operational Aerodynamic Data Book, Orbiter Vehicle Aerodynamic Data, Volume 3." Rockwell International, 1985.
7. Rockwell International. "Space Shuttle Ascent GN&C Data Book Appendix." Contract NAS9-18500. September 1992.
8. Roskam, J. *Airplane Flight Dynamics and Automatic Flight Controls*. Roskam Aviation and Engineering Corporation, Ottawa, Kansas, 1982.
9. Springer, A. "Initial Ascent and Entry Aerodynamic Database for the Wing/Body 001 (WB001) Reusable Launch Vehicle (RLV) Configuration." Memorandum, July 1994.

515-32

4978

**N95- 32433**

**SCANNERS, OPTICAL CHARACTER READERS, CYRILLIC  
ALPHABET AND RUSSIAN TRANSLATIONS**

**Final Report  
NASA/ASEE Summer Faculty Fellowship Program 1994  
Johnson Space Center**

<b>Prepared By:</b>	<b>Gordon G. Johnson, Ph.D.</b>
<b>Academic Rank:</b>	<b>Professor</b>
<b>College and Department:</b>	<b>University of Houston Department of Mathematics Houston, Texas 77204</b>
<b>NASA/JSC</b>	
<b>Directorate:</b>	<b>Information Systems</b>
<b>Division:</b>	<b>Technical Systems</b>
<b>Branch:</b>	<b>Client Server Systems</b>
<b>JSC Colleague:</b>	<b>Lui Wang</b>
<b>Date Submitted:</b>	<b>August 16, 1994</b>
<b>Contract Number:</b>	<b>NGT-44-005-803</b>